https://doi.org/10.48048/tis.2022.2557

Structure-Based Design and Molecular Simulations of Some Quercetin-Based Drugs as Repurposable Inhibitors of SARS-CoV-2 Main Protease

Yusuf Oloruntoyin Ayipo[1,2,*], Waleed A Alananzeh[1], Zuliah Abiola Abdulsalam[2], Umar Muhammad Badeggi[3], Akeem Adebayo Jimoh[2], Wahab Adesina Osunniran[2] and Mohd Nizam Mordi[1]

[1]Centre for Drug Research, Universiti Sains Malaysia, Gelugor 11800, Penang, Malaysia
[2]Department of Chemistry and Industrial Chemistry, Kwara State University, Malete, Ilorin, Nigeria
[3]Department of Chemistry, Ibrahim Badamasi Babangida University Lapai, Minna 4947, Nigeria

([*]Corresponding author's e-mail: yusuf.ayipo@kwasu.edu.ng)

Received: 9 February 2022, Revised: 15 March 2022, Accepted: 19 March 2022, Published: 31 October 2022

Abstract

In this study, virtual screening and molecular dynamics (MD) protocols were applied to screen 2826 FDA-approved natural product drugs from the Selleckchem.com library for prospective inhibitors of the SARS-CoV-2 main protease. From the virtual screening through HTVS, SP and XP docking analysis, hyperoside, rutin hydrate, rutoside and quercitrin displayed a stronger binding affinity with respective XP docking scores of –11.389, –11.340, –11.087 and –10.232 kcal/mol than co-crystallized N-[2-(5-fluoro-1H-indol-3-yl)ethyl]acetamide (HWH) and positive inhibitors, lopinavir and ritonavir which scored –5.493, –6.463 and –6.221 kcal/mol respectively. Selectively, the binding free energy, MMGB(SA) of hyperoside and rutin hydrate was observed as –21.55 and –25.82 kcal/mol respectively compared to lopinavir and ritonavir with –17.66 and –5.28 kcal/mol respectively. Consistently, the selected drugs displayed good thermodynamics conformational stability, thus, recommended as promising repurposable inhibitors of the SARS-CoV-2 main protease amenable for further studies.

Keywords: SARS-CoV-2 main protease, Molecular docking, Molecular dynamics, Quercetin, Natural repurposable drugs

Introduction

Severe acute respiratory syndrome coronavirus 2 (SARS-CoV-2) suddenly emerged around late 2019, thereby causing a global pandemic termed coronavirus 2019 (COVID-19). Since its zoonotic outbreak similar to the previous SARS-CoV-1 and Middle East respiratory syndrome CoV (MERS-CoV), it has destabilized global healthcare and economic systems through daily infections and loss of lives [1,2]. Although, the evolution of various vaccines has significantly doused the tensions of COVID-19 infection worldwide, however, there remains a challenge of accessibility to address the urgent situations, making a continuous search for effective therapeutics remain significant.

The viral main proteases (M^{pro}) of SARS-CoV-2 play pivotal roles in the modulation of viral life processes such as replication and transcription. The enzymes are strongly implicated in the proteolytic cleavage of viral polyproteins such as the pp1a and pp1b into intermediates or fully developed viral proteins including the nsp4-9 and nsp12-15, as such, representing plausible therapeutic targets [1,3,4]. Notably among the inhibitors of the target in clinical applications of COVID-19 include lopinavir and ritonavir, however, they are reportedly challenged by short-term efficacy, inability to reduce mortality and various degrees of aftereffects [5]. These make the continuous search for better alternatives remains important.

The scientific processes in modern drug design are cost-effectively managed and accelerated with the aid of computational molecular modelling, strategically, through ligand-based or structure-based design [6]. Molecular docking and molecular dynamics remain some of the most popular structure-based computational tools for an augmented and accelerated study of characteristic binding interactions of bioactive molecules to therapeutic targets as well as stability. Among the high-performance strategies, the workflow of high throughput screening integrates stratified ligand-receptor docking protocols, from high

throughput virtual screening (HTVS) to standard precision (SP) to extra precision (XP) modes. Molecular dynamics represents an indispensable tool for virtual biophysical and structural probes and is usually applied to evaluate the thermodynamic stability and flexibility of the selected drugs in complex with the receptor [7]. The application of these procedures in some previous studies successfully enriched the potent fractions and identified the most promising candidates for further study [8-10]. Although, some inhibitors of SARS-CoV-2 M^{pro} such as Mn-methisazone, lopinavir, ritonavir and tipranavir have been reported, however, they mostly showed unpleasant aftereffects at clinical levels [8,11,12]. Moreover, the cheaper and safer Food and Drug Administration- (FDA-)approved natural product drugs with established pharmacokinetics and druggability remains underexplored against the SARS-CoV-2 M^{pro}.

Thus, in this study, virtual screening through high throughput virtual screening (HTVS), standard precision (SP) and extra precision (XP) ligand-receptor docking simulations were applied to screen 2826 FDA-approved natural product drugs from the Selleckchem.com library for prospective inhibitors of SARS-CoV-2 M^{pro}. The selected drugs with stronger inhibitory potentials in comparison with co-crystallized ligand and reference inhibitors of SARS-CoV-2 M^{pro} in clinical trials were further evaluated for stability in complex with the receptor using computational molecular dynamics (MD) simulation protocols. The candidates with promising potentials an anti-SARS-CoV-2 through M^{pro} target were identified for further study.

Materials and methods

Dataset retrieval and ligand preparation for high throughput screening

A total number of 2826 FDA-approved natural product drugs were retrieved from the Selleckchem.com (https://www.selleckchem.com/) repurposing library in structure data file (SDF) format. The preparation of the ligands is importantly required for the correction of Lewis structures and removal of ligand mistakes to avoid downstream computational errors. To achieve these, the downloaded ligand files were imported into the workspace of Maestro 12.2 for preparation using the LigPrep module (LigPrep, Schrodinger, LCC, New York, NY, 2019). The preparation protocols entail the addition of hydrogens, Epik target energy minimization at pH of 7.0 ± 2.0 and conversion of 2D to 3D structures. These were followed by the estimation of geometry and partial atomic charges using optimized potentials for liquid simulation 3e (OPLS-3e) [13]. The generated minimised conformers with possible ionization states were saved in a ready-to-dock LigPrep.out file.

Protein preparation, receptor grid generation and analysis of receptor binding pocket

The X-ray resolved structure of SARS-CoV-2 main protease with a high resolution of 1.59 Å and 306 amino acid residues in complex with (N-[2-(5-fluoro-1H-indol-3-yl)ethyl]acetamide) (HWH) was retrieved from the Research Collaboratory for Structural Bioinformatics (RCSB) protein data bank (PDB 5R7Z) [2]. The structure was imported into the Maestro 12.2 workspace for preparation through preprocessing, filling of missing loops and assignment of protonation states using Protein Preparation wizard [14]. These were followed by optimization, refining and energy minimization for the conversion of heavy atoms to relative mean standard deviation (RMSD) 0.3 using the OPLS-3e force field of Maestro 12.12 [4,13]. The enclosing grid box was generated by the centroid of the workspace ligand, HWH with x, y and z coordinates of 19.07, –2.54 and 3.83 respectively and defaults settings of the ligand docking length within 20 Å, saved in gridbox.zip file. The accuracy of the receptor-binding pocket, essential for reliable docking procedures was analysed based on reported literature [2,15].

High throughput screening molecular docking

Computational workflows of ligand-receptor molecular docking simulation through HTVS to SP to XP modes were employed to enrich the potent fractions at each level towards identifying the most promising inhibitors of the selected receptor, adopting some reported protocols [6,16,17].

Molecular dynamics

The binding energy, stability and conformational flexibility of the selected ligand-receptor complex systems were evaluated along the trajectories of MD simulation using molecular mechanics (MM) force field in Ligand and Receptor Molecular Dynamics (LARMD) server-based software integrated with AMBER 16 force field [18,19]. The PDB file of each complex was uploaded for simulation with default all-atom MD set at 3000 ps, water implicit “Int-mode”. The statistics of the H-bonding plot shows the H-bond contacts that occurred between the amino acid residues and drug molecules during the simulation. The RMSD plot indicates the deviation of the average distance of the atoms of the receptor/ligands from

their original positions while the radius of gyration reveals the RMS distance between each atom of the receptor to their control. The possible conformational dynamics of each complex system and energetics of the binding ligands were assessed by capturing the transition states of the receptor with a folding free energy barrier, displayed as the fractions of native contacts. The fluctuations/isotropic displacements that occurred on each amino acid residue along the simulation trajectories were represented by the RMS fluctuation (RMSF). Molecular Mechanics Generalized Born Surface Area continuum solvation [MM/GB(SA)] re-scoring methods and the statistics of hydrogen bonds between the bound ligands and the protein residues depict the ligand-receptor binding affinities and binding free energies. The MM/GB(SA) was calculated as ΔG_{bind} using the equations below:

$$\Delta G_{bind} = G_{complex} - G_{receptor} - G_{ligand} \quad (1)$$

$$= \Delta H - T\Delta S \approx \Delta E_{gas} + \Delta G_{sol} + T\Delta S \quad (2)$$

$$\Delta E_{gas} = \Delta E_{int} + \Delta E_{ele} + \Delta E_{vdw} \quad (3)$$

$$\Delta G_{sol} = \Delta G_{GB} + \Delta G_{surf} \quad (4)$$

Where ΔE_{gas} = gas-phase energy change, ΔE_{int} = change in internal energy, ΔE_{ele} = electrostatic force, ΔE_{vdw} = change in van der Waals forces, ΔG_{sol} = solvation free energy, ΔG_{surf} = non-polar contribution to the solvation-accessible surface area (SASA) [4,19-22].

Final hits

The drug molecules that demonstrate the strongest inhibitory potentials against the SARS-CoV-2 M^{pro} and better thermodynamics stability in comparison with the referenced lopinavir and ritonavir are selected as final hits and recommended for further experimental studies.

Results and discussion

Analysis of receptor binding pocket

The accuracy of the predicted ligand-protein binding site provides a great insight into the biological functions of the protein and significantly aid structure-based drug designs [23]. According to the depositors of the crystal structure, the active site SARS-CoV-2 main protease (PDB 5R7Z) is sandwiched between the 2 β-barrel domains I and II consisting of amino acid residues in positions 10 - 99 and 100 - 182 respectively. Residues 198 - 306 form domain III with a bundle of α-helices proposedly for dimerization modulation while Hie 41 and Cys 145 constitute the catalytic dyad with the active site completion by Ser 1 and Glu 166 interplay [2]. Similarly, experimental studies have shown that the SARS-CoV-2 M^{pro} consists of side-chain residues, His 41, Val 42, Thr 25, Asn 119, Phe 140, Asn 142, Ser 144, Cys 145, His 163 and Glu 166 while Thr 26, Leu 141, Gly 143, His 164 and Met 165 form the backbone residues [15]. Consistently, the active site predicted by selecting the centroid of the workspace co-crystallized HWH ligand contains the amino acid highlighted residues, although, only the interactive ones with the co-crystallized HWH and rutin were labelled (**Figure 1**(**A**)). The 3D ball and stick models (**Figure 1**(**B**)) also support the accurate detection of receptor binding pocket and interactions of the selected drugs and references with pharmacological amino acid residues in the active site.

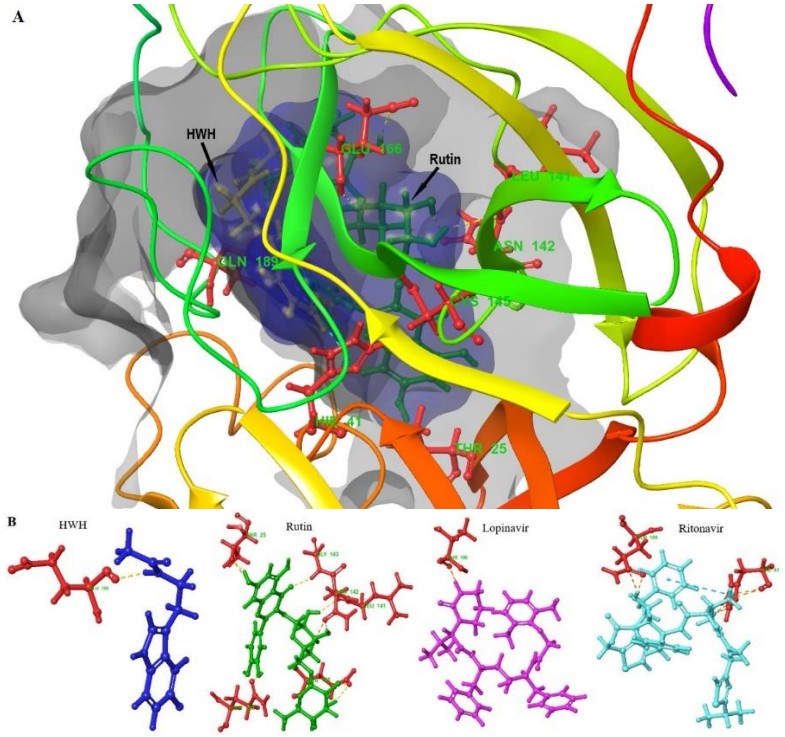

Figure 1 3D Poses of rutin and selected references at the active site of SARS-CoV-2 M^{pro}: (A) The surface of the active site (blue solid) with docked rutin (green ball and stick model) and co-crystallized HWH (yellow ball and stick model) occupy a similar binding sub-pocket. (B) Bonding interactions of co-crystallized HWH, rutin and selected references with amino acid residues at the active binding pocket of the receptor. Rutin exhibited more hydrophilic interactions with active amino acid residues than co-crystallized HWH and the references, lopinavir and ritonavir.

High throughput screening molecular docking

Complete virtual screening was conducted through molecular docking simulations for enriching the fraction of promising inhibitors through binding affinity predictions. The precision, accuracy and reproducibility of the adopted docking protocols were validated through redocking of the co-crystallized HWH within the active pocket of the receptor and computing its RMSD in comparison with the retrieved crystal complex from RCSB PDB. An RMSD value of 0.5 Å obtained validated the protocols as good [24,25]. The protocols incorporated stratified analysis starting with HTVS of 5786 conformers generated from the LigPrep of a total of 2826 FDA-approved natural product drugs. After sorting the results in ascending order of docking scores (kcal/mol) and removal of duplicates, the top-ranked 100 drug conformers were selected for SP docking. The 7 top-ranked drug conformers with the highest SP docking scores were selected for a more discriminate, robust torsional refinement and ligand screening XP docking. This provides an opportunity for precision, accuracy and reproducibility of the screening protocols, although, more time-consuming and requires highly computing wares [26]. The selected docked drugs were ranked based on the algorithms of docking XP scores (**Table 1**). From the results, the co-crystallized HWH ligand displayed HTVS, SP and XP docking scores of –6.497, –7.047 and –5.493 kcal/mol respectively. Selectively, the top-ranked drug, hyperoside showed a consistent highest binding affinity respectively as –7.341, –8.214 and –11.389 kcal/mol along with the screening protocols, followed by other 3 members of quercetin flavonoids, rutin hydrate, rutoside and quercitrin, then daidzin, a selective inhibitor of aldehyde dehydrogenase (ALDH-2) [27] and ioversol, an organoiodine clinical diagnostic agent [28] and alogliptin, a DPP-4 inhibitor antidiabetic [29]. The 2 reference inhibitors of M^{pro} in clinical trials of COVID-19, lopinavir and ritonavir [11] scored far below the 7 selected drugs. These were supported by the glide binding energy scores and indicate potentials for stronger inhibitory effects of the selected drugs against the SARS-CoV-2 M^{pro} in comparison with HWH, lopinavir and ritonavir.

Table 1 Results of virtual screening molecular docking simulations of selected drugs.

Name	HTVS score (kcal/mol)	SP score (kcal/mol)	XP score (kcal/mol)	Glide energy (kcal/mol)	Interactions	
					H-bond	π – π
Hyperoside	–7.341	–8.214	–11.389	–50.796	Hie 41, Phe 140, Gly 143, Glu 166, Arg 188	-
Rutin hydrate	–7.896	–7.452	–11.340	–67.348	Thr 25, Leu 141, Asn 142, Gly 143, Glu 166, Gln 189	-
Rutin (Rutoside)	–7.097	–8.153	–11.087	–70.546	Thr 25, Leu 141, Gly 143, Glu 166	-
Quercitrin	–7.615	–8.403	–10.232	–65.040	Phe 140, Asn 142, Gly 143, Glu 166, Arg 188	-
Daidzin	–7.542	–7.825	–9.318	–52.351	Thr 26, Glu 166, Thr 190	-
Ioversol	–8.122	–7.584	–8.868	–62.615	Asn 142, Glu 166, Arg 188, Thr 190	-
Alogliptin	–6.933	–8.424	–7.575	–45.074	Hie 41, Cys 44, Gly 143, Glu 166	Hie 41
Lopinavir	–5.504	–7.161	–6.463	–51.552	Thr 190	-
Ritonavir	–6.763	–6.374	–6.221	–64.593	Gln189	Hie 41
HWH	–6.497	–7.047	–5.493	–33.996	Glu 166	-

From the binding poses (**Figure 2**), the co-crystallized HWH, referenced lopinavir and ritonavir displayed only 1 hydrophilic interaction each through Glu 166, Thr 190 and Gln 189 respectively. Only HWH showed additional hydrophobic interaction to Hie 41. The selected 7 drugs demonstrated more hydrophilic H-bonding interactions between 4 - 6 to various amino acid residues essential for pharmacological expression of the receptor. For instance, the 2 top-ranked drugs, hyperoside and rutin hydrate interacted through hydrogen bonds to Thr 25, Hie 41, Phe 140, Asn 142 and Glu 166 which constitute the side chains of the receptor. They also showed hydrophilic interactions to some backbone residues, Leu 141 and Gly 143. Only alogliptin showed aromatic π – π interaction to Hie 41 consistently with ritonavir, other selected drugs as well as the references displayed non-bonding van der Waals interactions with other important amino acid residues in the active pocket of the receptor as displayed in the 2D binding poses (**Figure 2**). The selected drugs are polyphenol secondary metabolites that are naturally endowed with pleiotropic effects. Their structures consist of more than 1 phenolic ring which favours a network of H-bonding with amino acid residues of the protein structure. The aromatic rings are also potential pharmacophores for hydrophobic interactions with alkyl groups of amino acids, while the irreversible covalent bonds from the intermolecular interactions stabilise the resultant phenol-protein complexes. These further support their strong binding affinity within the active subsites 1 and 2 of the receptor, consistently with some reported inhibitors [15,30,31], and indicate their promising inhibitory effects against M^{pro} as a therapeutic pathway for mitigating SARS-CoV-2 replication.

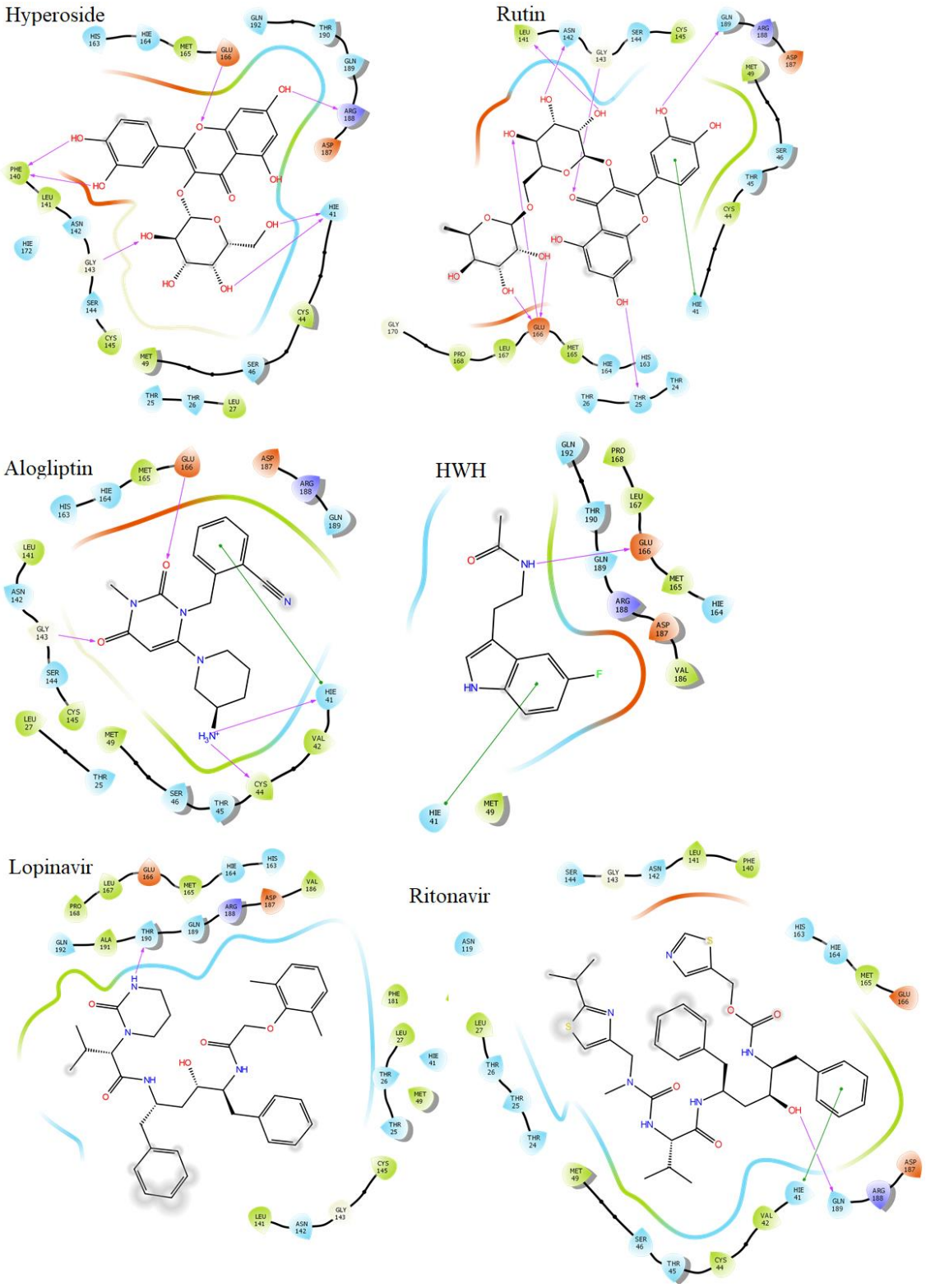

Figure 2 2D Illustration of binding poses showing interactions of the selected drugs and references with active amino acid residues. Hydrogen bond (magenta arrow); π – π interaction (green line).

Molecular dynamics

The MD, an indispensable tool for virtual biophysical and structural probes [7] was used to evaluate the thermodynamic stability and flexibility of the selected drugs in complex with the receptor. Two drugs hyperoside and rutin hydrate (representing the quercetin flavonoids, rutin hydrate, rutoside and quercitrin) were selected for MD simulation in comparison with lopinavir and ritonavir. From the results (**Table 2**), the total binding free energy, MMGB(SA) estimated by a sum of GBT and TS comprehensively quantifies the conformational interactions that occurred between the selected drugs and the SARS-CoV-2 M^{pro} along the trajectories of MD simulations. The results indicate higher binding free energies and affinities of hyperoside and rutin hydrate to the receptor than lopinavir and ritonavir, renowned inhibitors of SARS-CoV-2 M^{pro} in clinical trials [32], consistently with the virtual screening scores. The statistics of the H-bond (**Figure 3**(**A**)) shows that the selected hyperoside and rutin hydrate exhibited a higher number of H-bond contacts than the references, lopinavir and ritonavir during the simulations. This contributively accounts for their higher binding affinities to the receptor than the references. Similarly, the affinity-inclined contributions of other complementary electrostatic/hydrophobic bonding and non-bonding van der Waals interactions to other polar and non-polar amino acid residues respectively cannot be overruled. The emphasis of these interactions is essential for promising druggability and pharmacological expressions with the receptor [33]. The RMSD plots (**Figure 3**(**B**)) indicates that the receptor backbone initially experienced slight atomic deviation and became equilibrated just after the simulation commenced (<100 ps) and subsequently maintain stability with an insignificant deviation of <1.0 Å till the end of the simulation. The 2 selected drugs, hyperoside and rutin hydrate mostly entered the equilibrium condition around the same time and maintained stability throughout the simulations, although, rutin hydrate displayed the highest stability while the least is observed with ritonavir. Averagely, good thermodynamic stabilities were observed for hyperoside and rutin hydrate consistently support their strong inhibitory binding effects with the receptor in better terms than lopinavir and ritonavir.

Table 2 Binding free energy of selected drugs and references.

Drug	ELE	VDW	GAS	GBSOL	GBTOT	TS	ΔGB
Hyperoside	–14.89	–54.57	–69.46	25.65	–43.82	22.27	–21.55
Rutin	–16.68	–65.25	–81.87	31.39	–50.58	24.76	–25.82
Lopinavir	–4.36	–48.08	–47.45	12.60	–34.84	17.18	–17.66
Ritonavir	–9.11	–38.04	–47.14	17.91	–29.24	23.96	–5.28

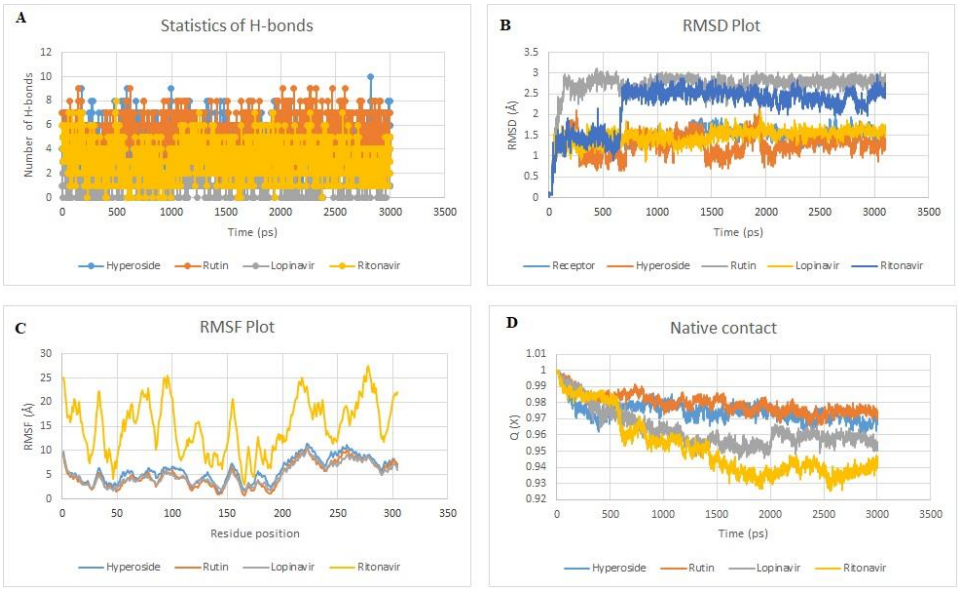

Figure 3 Molecular dynamics conformations for affinity and stability: (A) Statistics of H-bond contacts, (B) RMSD plot, (C) RMSF plot and (D) Native contact. Hyperoside and rutin experienced more H-bond contacts, higher stability with diminutive fluctuations than lopinavir and ritonavir along the trajectories of simulation.

The RMSF plot representing the mean square isotropic displacements, dynamic thermal motion paths and transient channels that support the ligands to enter the internal binding cavities of the receptor is presented (**Figure 3**(**C**)). The 2 selected drugs, hyperoside and rutin hydrate demonstrated good stability, indicated by diminutive fluctuation consistently with lopinavir but in better terms than ritonavir. Since flexibility significantly contributes to thermodynamic stability, resistance to change in environment and the binding/interaction potentials of protein receptors to ligands, it could be inferred that the enhanced thermodynamic stability observably influenced by the selected drugs is due to their ideal flexibility. These interestingly contribute to the integrity and the predisposition of the target in the pathogenesis of SARS-CoV-2 infection [34]. The native contact captures the transition states between the selected ligands as well as the reference drugs and the receptor with a folding free energy barrier indicate thermostability of the complexes. A system comprising of an unfolding protein is indicated by a large fluctuation in Q (X). Considering the result (**Figure 3**(**D**)), the drugs under focus, hyperoside and rutin hydrate displayed the least change in Q compared to lopinavir, while the highest (unstable) is observed with ritonavir, consistently with previous results. To further probe the structure-related influences of the ligands, the compactness and stability of the selected ligand-receptor complexes were studied through the radius of gyration (Rg) plot (**Figure 4**). The Rg is determined by the folding state of protein receptors in complexes with the ligands along the trajectories of simulations [19]. The selected drugs, hyperoside and rutin hydrate are more favoured by good compactness and stability than lopinavir, while ritonavir remains most perturbed. Although, the trajectory of MD simulations could be extended to a longer time in subsequent studies to affirm the validity of the promising implications. However, the present results provide firsthand confidence for embarking on other rigorous and costly assessments selectively for the identified natural product drugs.

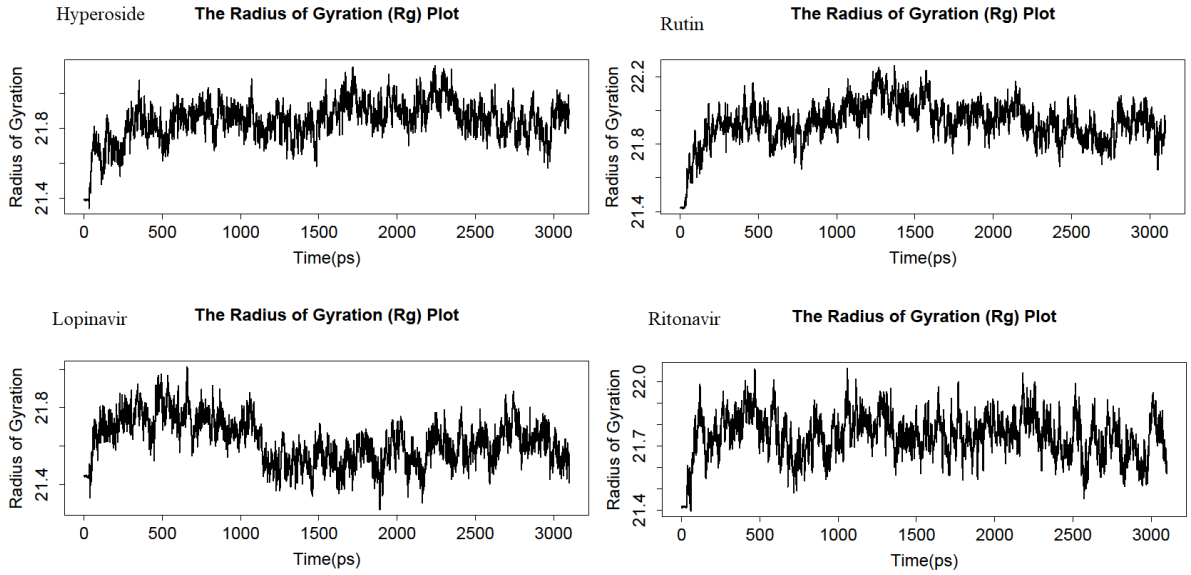

Figure 4 The radius of gyration plots of selected drugs and references. Hyperoside and rutin were less perturbed during simulation consistently with lopinavir while ritonavir showed the highest perturbation.

Final hits

From the virtual screening molecular docking and MD simulations, the natural product drugs with consistent inhibitory binding affinities, thermodynamic stability and ideal flexibility with the receptor were selected as final hits. These include hyperoside, rutin hydrate, rutin (rutoside) and quercitrin (**Figure 5**). Interestingly, SARS-CoV-2 reportedly causes inflammatory pneumonia in COVID-19 patients with high mortality implicated by cytokine storms. The severity of the SARS-CoV-2-mediated inflammation is responsible for some major life-threatening conditions of COVID-19 [35]. Moreover, several experimental studies have validated the quercetin flavonoids, specifically hyperoside and quercetin analogues including rutin and quercetin as a potent anti-inflammatory, antioxidant and antithrombotic agents in clinical trials for COVID-19 comorbidities [3]. They express various mechanisms of action including the inhibition of arachidonic acid- and croton oil-induced oedema, inhibition of cyclooxygenase 2 and hyaluronidase enzymes, suppression of interleukin-6, NO and tumour necrosis factor production as well as the NF-kb

signalling pathway [35,36]. They are present in vast natural products including the plants of the genera Hypericum and Crataegus as well as various fruits and vegetables such as citrus, apple, onion and buckwheat [37]. Thus, they represent promising inhibitors of SARS-CoV-2 M^{pro}-inclined replication and suppressors of the inflammatory pathways of COVID-19.

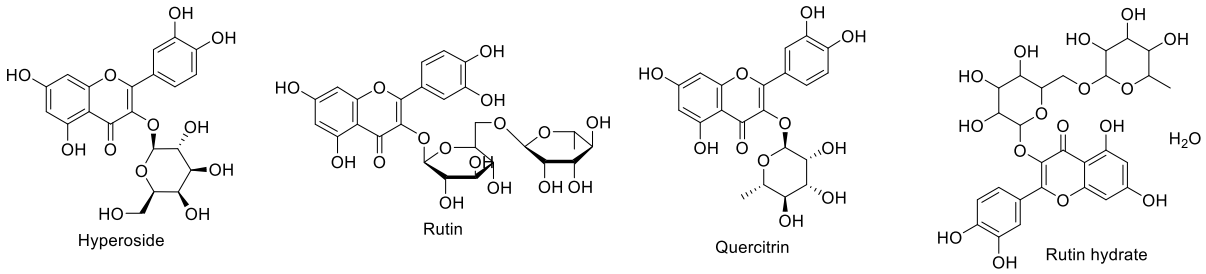

Figure 5 Chemical structures of finally identified promising quercetin-based inhibitors SARS-CoV-2 M^{pro}.

Conclusions

The Glide complete solution virtual screening protocols incorporating HTVS, SP and XP modes of stratified molecular docking simulations has aided the screening of the 2826 FDA-approved natural product drugs from the Selleckchem.com repurposing library to identify promising inhibitors of SARS-CoV-2 M^{pro}. Several drugs namely, hyperoside, rutin hydrate, rutoside, quercitrin, daidzin, ioversol and alogliptin consistently demonstrated stronger binding affinity to the receptor to the references, co-crystallized HWH and, lopinavir-ritonavir, inhibitors of SARS-CoV-2 M^{pro} in clinical trials. The top-ranked drugs, hyperoside and rutin which represents rutin hydrate, rutoside and quercitrin displayed better flexibility and thermodynamic stability upon MD simulation in comparison with lopinavir and ritonavir.

More interestingly, some reported experimental models have validated their candidacy as promising inhibitors of SARS-CoV-2 M^{pro} as well as suppressors of inflammatory signalling pathways of COVID-19. Subsequently, rutin, rutoside and other glucoside flavonoids of quercetin analogues are currently in clinical studies of COVID-19. The cumulative application of computational virtual screening and MD simulations in this study has demonstrated cheaper, faster and environmentally approaches towards the structure-based design of potent anti-SARS-CoV-2 therapeutic candidates from vast natural products. Although, further experimental studies are essential for the confirmation of their bona fide anti-SARS-CoV-2 activity through *in vitro* and *in vivo* models, however, hyperoside, rutin hydrate, rutoside and quercitrin represent promising inhibitors of SARS-CoV-2 amenable for further translational studies.

Acknowledgements

This work was financially supported by Tertiary Education Fund Nigeria, Fundamental Research Grant Scheme, Ministry of Higher Education of Malaysia (Grant no. 203.CDADAH.6711955) and Universiti Sains Malaysia GA Scheme (Grant no. 308.AIPS.415401).

References

[1] K Amporndanai, X Meng, W Shang, Z Jin, M Rogers, Y Zhao, Z Rao, ZJ Liu, H Yang, L Zhang, PM O'Neill and SS Hasnain. Inhibition mechanism of SARS-CoV-2 main protease by ebselen and its derivatives. *Nat. Commun*. 2021; **12**, 3061.

[2] A Douangamath, D Fearon, P Gehrtz, T Krojer, P Lukacik, CD Owen, E Resnick, C Strain-Damerell, A Aimon, P Ábrányi-Balogh, J Brandão-Neto, A Carbery, G Davison, A Dias, TD Downes, L Dunnett, M Fairhead, JD Firth, SP Jones, … MA Walsh. Crystallographic and electrophilic fragment screening of the SARS-CoV-2 main protease. *Nat. Commun*. 2020; **11**, 5047.

[3] YO Ayipo, SN Yahaya, WA Alananzeh, HF Babamale and MN Mordi. Pathomechanisms, therapeutic targets and potent inhibitors of some beta-coronaviruses from bench-to-bedside. *Infect. Genet. Evol.* 2021; **93**, 104944.

[4] YO Ayipo, I Ahmad, YS Najib, SK Sheu, H Patel and MN Mordi. Molecular modelling and structure-activity relationship of a natural derivative of o-hydroxybenzoate as a potent inhibitor of dual NSP3 and NSP12 of SARS-CoV-2: *in silico* study. *J. Biomol. Struct. Dyn.* 2022. DOI: 10.1080/07391102.

2022.2026818.

[5] Recovery Collaborative Group. Lopinavir-ritonavir in patients admitted to hospital with COVID-19 (RECOVERY): A randomised, controlled, open-label, platform trial. *Lancet* 2020; **396**, 1345-52.

[6] V Asati, SS Thakur, N Upmanyu and SK Bharti. Virtual screening, molecular docking, and DFT studies of some thiazolidine-2,4-diones as potential PIM-1 kinase inhibitors. *ChemistrySelect* 2018; **3**, 127-35.

[7] DL Lynch, DP Hurst, DM Shore, MC Pitman and PH Reggio. Molecular dynamics methodologies for probing cannabinoid ligand/receptor interaction. *Methods Enzymol.* 2017; **593**, 449-90.

[8] AAAMM Alkhatip, M Georgakis, LRM Valenzuela, M Hamza, E Farag, J Hodgkinson, H Hosny, AM Kamal, M Wagih, A Naguib, H Yassin, H Algameel, M Elayashy, M Abdelhaq, MI Younis, H Mohamed, M Abdulshafi and MA Elramely. Metal-bound methisazone; novel drugs targeting prophylaxis and treatment of sars-cov-2, a molecular docking study. *Int. J. Mol. Sci.* 2021; **22**, 2977.

[9] RA Friesner, JL Banks, RB Murphy, TA Halgren, JJ Klicic, DT Mainz, MP Repasky, EH Knoll, M Shelley, JK Perry, DE Shaw, P Francis and PS Shenkin. Glide: A new approach for rapid, accurate docking and scoring. 1. method and assessment of docking accuracy. *J. Med. Chem*. 2004; **47**, 1739-49.

[10] TA Halgren, RB Murphy, RA Friesner, HS Beard, LL Frye, WT Pollard and JL Banks. Glide: A new approach for rapid, accurate docking and scoring. 2. enrichment factors in database screening. *J. Med. Chem*. 2004; **47**, 1750-9.

[11] W Cui, K Yang and H Yang. Recent progress in the drug development targeting SARS-CoV-2 main protease as treatment for COVID-19. *Front. Mol. Biosci*. 2020; **7**, 616341.

[12] Y Kumar, H Singh and CN Patel. In silico prediction of potential inhibitors for the main protease of SARS-CoV-2 using molecular docking and dynamics simulation-based drug-repurposing. *J. Infect. Public Health* 2020; **13**, 1210-23.

[13] E Harder, W Damm, J Maple, C Wu, M Reboul, JY Xiang, L Wang, D Lupyan, MK Dahlgren, JL Knight, JW Kaus, DS Cerutti, G Krilov, WL Jorgensen, R Abel and RA Friesner. OPLS3: A force field providing broad coverage of drug-like small molecules and proteins. *J. Chem. Theory Comput*. 2016; **12**, 281-96.

[14] GM Sastry, M Adzhigirey, T Day, R Annabhimoju and W Sherman. Protein and ligand preparation: Parameters, protocols, and influence on virtual screening enrichments. *J. Comput. Aided Mol. Des*. 2013; **27**, 221-34.

[15] SV Stoddard, SD Stoddard, BK Oelkers, K Fitts, K Whalum, K Whalum, AD Hemphill, J Manikonda, LM Martinez, EG Riley, CM Roof, N Sarwar, DM Thomas, E Ulmer, FE Wallace, P Pandey and S Roy. Optimization rules for SARS-CoV-2 Mpro antivirals: Ensemble docking and exploration of the coronavirus protease active site. *Viruses* 2020; **12**, 942.

[16] M Luo, H Wang, Y Zou, S Zhang, J Xiao, G Jiang, Y Zhang and Y Lai. Identification of phenoxy acetamide derivatives as novel DOT1L inhibitors via docking screening and molecular dynamics simulation. *J. Mol. Graph. Model.* 2016; **68**, 128-39.

[17] GK Veeramachaneni, KK Raj, LM Chalasani, JS Bondili and VR Talluri. High-throughput virtual screening with e-pharmacophore and molecular simulations study in the designing of pancreatic lipase inhibitors. *Drug Des. Devel. Ther*. 2015; **9**, 4397-412.

[18] JF Yang, F Wang, YZ Chen, GF Hao and GF Yang. LARMD: Integration of bioinformatic resources to profile ligand-driven protein dynamics with a case on the activation of the estrogen receptor. *Brief Bioinform*. 2019; **21**, 2206-18.

[19] YO Ayipo, SN Yahaya, HF Babamale, I Ahmad, H Patel and MN Mordi. β-Carboline alkaloids induce structural plasticity and inhibition of SARS-CoV-2 nsp3 macrodomain more potently than remdesivir metabolite GS-441524: Computational approach. *Turk. J. Biol.* 2021; **45**, 503-17.

[20] Z Babar, M Khan, M Zahra, M Anwar, K Noor, HF Hashmi, M Suleman, M Waseem, A Shah, S Ali and SS Ali. Drug similarity and structure-based screening of medicinal compounds to target macrodomain- I from SARS-CoV-2 to rescue the host immune system: A molecular dynamics study. *J. Biomol. Struct. Dyn.* 2020; **40**, 523-37.

[21] S Genheden and U Ryde. The MM/PBSA and MM/GBSA methods to estimate ligand-binding affinities. *Expert Opin. Drug Discov*. 2015; **10**, 449-61.

[22] E Wang, H Sun, J Wang, Z Wang, H Liu, JZH Zhang and T Hou. End-point binding free energy calculation with MM/PBSA and MM/GBSA: Strategies and applications in drug design. *Chem. Rev.* 2019; **119**, 9478-508.

[23] J Zhao, Y Cao and L Zhang. Exploring the computational methods for protein-ligand binding site prediction. *Comput. Struct. Biotechnol. J*. 2020; **18**, 417-26.

[24] A Castro-Alvarez, AM Costa and J Vilarrasa. The performance of several docking programs at reproducing protein-macrolide-like crystal structures. *Molecules* 2017; **22**, 136.
[25] D Ramírez and J Caballero. Is it reliable to take the molecular docking top scoring position as the best solution without considering available structural data? *Molecules* 2018; **23**, 1038.
[26] P Parmar, P Rao, A Sharma, A Shukla, RM Rawal, M Saraf, BV Patel and D Goswami. Meticulous assessment of natural compounds from NPASS database for identifying analogue of GRL0617, the only known inhibitor for SARS-CoV2 papain-like protease (PLpro) using rigorous computational workflow. *Mol. Divers.* 2022; **26**, 389-407.
[27] CS Silva, GV Portari and H Vannucchi. *Antioxidant treatment and alcoholism*. *In*: VB Patel (Ed.). Molecular aspects of alcohol and nutrition. Academic Press, London, 2016, p. 119-31.
[28] JK Aronson. *Iodinated contrast media*. *In*: Meyler's side effects of drugs. 16th eds. Elsevier Science, Amsterdam, The Netherlands, 2016, p. 239-97.
[29] JM Terrell and TF Jacobs. *Alogliptin*. *In*: StatPearls: Content is king. StatPearls Publishing, Treasure Island, Florida, 2021, Available at: https://www.ncbi.nlm.nih.gov/books/NBK507809, accessed January 2022.
[30] T Dai, J Chen, DJ McClements, P Hu, X Ye, C Liu and T Li. Protein-polyphenol interactions enhance the antioxidant capacity of phenolics: Analysis of rice glutelin-procyanidin dimer interactions. *Food Funct*. 2019; **10**, 765-74.
[31] L Seczyk, M Swieca, I Kapusta and U Gawlik-Dziki. Protein-phenolic interactions as a factor affecting the physicochemical properties of white bean proteins. *Molecules* 2019; **24**, 408.
[32] U.S. National Library of Medicine. Clinical trials on lopinavir and ritonavir for COVID-19. 2021, Available at: https://www.clinicaltrials.gov/ct2/results?cond=Covid19&term=lopinavir&cntry=&state=&city=&dist =, accessed June 2021.
[33] G Klebe. *Protein-ligand interactions as the basis for drug action. In*: G Klebe (Ed.). Drug design. Springer, Berlin, Heidenberg, Germany, 2013, p. 61-88.
[34] AS Panja, S Maiti and B Bandyopadhyay. Protein stability governed by its structural plasticity is inferred by physicochemical factors and salt bridges. *Sci. Rep*. 2020; **10**, 1822.
[35] A Saeedi-boroujeni and MR Mahmoudian-Sani. Anti-inflammatory potential of Quercetin in COVID-19 treatment. *J. Inflamm*. 2021; **18**, 3.
[36] R Shukla, V Pandey, GP Vadnere and S Lodhi. *Role of flavonoids in management of inflammatory disorders*. *In*: VR Preedy (Ed.). Bioactive food as dietary interventions for arthritis and related inflammatory diseases. 2nd eds. Academic Press, London, 2019, p. 293-322.
[37] RJ Horwitz. *The allergic patient*. *In*: Integrative medicine. 4th eds. Elsevier, Amsterdam, The Netherlands, 2018, p. 300-9.